Correlated 0.01Hz - 40 Hz seismic and Newtonian noise and its impact on future gravitational-wave detectors

Kamiel Janssens,[1,2] Guillaume Boileau,[3] Nelson Christensen,[2] Nick van Remortel,[1] Francesca Badaracco,[4,5] Benjamin Canuel,[6] Alessandro Cardini,[7] Andrea Contu,[7] Michael W. Coughlin,[8] Jean-Baptiste Decitre,[9] Rosario De Rosa,[10,11] Matteo Di Giovanni,[12,13] Domenico D'Urso,[14,7] Stéphane Gaffet,[9] Carlo Giunchi,[15] Jan Harms,[16,17] Soumen Koley,[16,17] Valentina Mangano,[13] Luca Naticchioni,[13] Marco Olivieri,[18] Federico Paoletti,[19] Davide Rozza,[14,7] Dylan O. Sabulsky,[9] Shahar Shani-Kadmiel,[20] and Lucia Trozzo[11]

[1] *Universiteit Antwerpen, Prinsstraat 13, 2000 Antwerpen, Belgium*
[2] *Université Côte d'Azur, Observatoire de la Côte d'Azur, CNRS, Artemis, 06304 Nice, France*
[3] *Université Côte d'Azur, Observatoire de la Côte d'Azur, CNRS, Laboratoire Lagrange, 06304 Nice, France*
[4] *Università degli studi di Genova, via Dodecaneso 33, 16146, Italy*
[5] *INFN, Sez. di Genova, via Dodecaneso 33, 16146, Italy*
[6] *LP2N, Laboratoire Photonique, Numérique et Nanosciences, Université Bordeaux–IOGS–CNRS:UMR 5298, rue F. Mitterrand, F–33400 Talence, France*
[7] *INFN, sezione di Cagliari, I-09042, Monserrato (Cagliari), Italy*
[8] *School of Physics and Astronomy, University of Minnesota, Minneapolis, Minnesota 55455, USA*
[9] *Laboratoire Souterrain à Bas Bruit (LSBB), CNRS: UAR3538, Avignon University, Rustrel F-84400,France*
[10] *Universitá Federico II Napoli, 80126 Napoli, Italy*
[11] *INFN - sezione di Napoli, 80126 Napoli, Italy*
[12] *La Sapienza Università di Roma, I-00185 Roma, Italy*
[13] *INFN, Sezione di Roma, I-00185 Roma, Italy*
[14] *Department of Chemistry, Physics, Mathematics and Natural Science, Università degli Studi di Sassari, I-07100, Sassari, Italy*
[15] *Istituto Nazionale di Geofisica e Vulcanologia, Sezione di Pisa, Italy*
[16] *Gran Sasso Science Institute (GSSI), I-67100 L'Aquila, Italy*
[17] *INFN, Laboratori Nazionali del Gran Sasso, I-67100 Assergi, Italy*
[18] *Sezione di Bologna, Istituto Nazionale di Geofisica e Vulcanologia, Bologna, Italy*
[19] *INFN - sezione di Pisa, 56127 Pisa, Italy*
[20] *R&D Department of Seismology and Acoustics, KNMI, De Bilt, The Netherlands*

(Dated: February 28, 2024)

We report correlations in underground seismic measurements with horizontal separations of several hundreds of meters to a few kilometers in the frequency range 0.01 Hz to 40 Hz. These seismic correlations could threaten science goals of planned interferometric gravitational-wave detectors such as the Einstein Telescope as well as atom interferometers such as MIGA and ELGAR. We use seismic measurements from four different sites, i.e. the former Homestake mine (USA) as well as two candidate sites for the Einstein Telescope, Sos Enattos (IT) and Euregio Maas-Rhein (NL-BE-DE) and the site housing the MIGA detector, LSBB (FR). At all sites, we observe significant coherence for at least 50% of the time in the majority of the frequency region of interest. Based on the observed correlations in the seismic fields, we predict levels of correlated Newtonian noise from body waves. We project the effect of correlated Newtonian noise from body waves on the capabilities of the triangular design of the Einstein Telescope's to observe an isotropic gravitational-wave background (GWB) and find that, even in case of the most quiet site, its sensitivity will be affected up to ∼20 Hz. The resolvable amplitude of a GWB signal with a negatively sloped power-law behaviour would be reduced by several orders of magnitude. However, the resolvability of a power-law signal with a slope of e.g. $\alpha = 0$ ($\alpha = 2/3$) would be more moderately affected by a factor ∼ 6-9 (∼3-4) in case of a low noise environment. Furthermore, we bolster confidence in our results by showing that transient noise features have a limited impact on the presented results.

I. INTRODUCTION

Searches for unmodeled and/or long duration gravitational-wave (GW) signals, such as the isotropic GW background (GWB) [1], are more susceptible to be biased by correlated noise. One such example are correlations in magnetic field fluctuations over Earth-scale distances, such as the Schumann resonances [2, 3]. Their potential effect on GWB searches with Earth-based GW interferometers – LIGO [4], Virgo [5] and KAGRA [6] – has been extensively investigated [7–14]. Moreover, the effect of correlated lightning glitches on searches for GW bursts, such as core collapse supernova, was studied [14, 15]. Furthermore, the effect of Schumann resonances on the Einstein Telescope (ET) was investigated [16] and shown to be a limiting noise source for the search for a GWB below ∼ 30Hz, in case ET has a similar magnetic coupling as LIGO/Virgo.

ET is the European proposal for a third-generation,

Deep Learning-based Kinetic Analysis in Paper-based Analytical Cartridges Integrated with Field-effect Transistors

Hyun-June Jang[1,2]‡, Hyou-Arm Joung[3]‡, Artem Goncharov[3], Anastasia Gant Kanegusuku[4], Clarence W. Chan[5], Kiang-Teck Jerry Yeo[5,6], Wen Zhuang[1,2], Aydogan Ozcan[3,7,8,9*], Junhong Chen[1,2*]

[1]Pritzker School of Molecular Engineering, University of Chicago, Chicago, IL 60637, USA

[2]Chemical Sciences and Engineering Division, Physical Sciences and Engineering Directorate, Argonne National Laboratory, Lemont, IL 60439, USA

[3]Department of Electrical and Computer Engineering, University of California, Los Angeles, CA 90095, USA

[4]Department of Pathology and Laboratory Medicine, Loyola University Medical Center, Maywood, IL 60153

[5]Department of Pathology, The University of Chicago, Chicago, IL 60637, USA

[6]Pritzker School of Medicine, The University of Chicago, Chicago, IL 60637, USA

[7]Department of Bioengineering, University of California, Los Angeles, CA 90095, USA

[8]California NanoSystems Institute (CNSI), University of California, Los Angeles, CA 90095, USA

[9]Department of Surgery, David Geffen School of Medicine, University of California, Los Angeles, CA 90095, USA

‡These authors contributed equally to this work

*Correspondence: ozcan@ucla.edu, junhongchen@uchicago.edu

Keywords: FET Biosensors, Paper Cartridge, Dry Chemistry, Deep Learning, Cholesterol

Capacitive coupling study of the HERD SCD prototype: preliminary results

Ruo-Si Lu, Rui Qiao, Ke Gong, Wen-Xi Peng, Wei-Shuai Zhang, Dong-Ya Guo, Jia-Ju Wei, Yi-Ming Hu, Jian-Hua Guo, Qi Wu, Peng Hu, Xuan Liu, Bing Lu, Yi-Rong Zhang

***Abstract*—The Silicon Charge Detector (SCD) is a subdetector of the High Energy Cosmic Radiation Detection payload. The dynamic range of the silicon microstrip detector can be extended by the capacitive coupling effect, which is related to the interstrip capacitance and the coupling capacitance. A detector prototype with several sets of parameters was designed and tested in the ion beams at the CERN Super Proton Synchrotron. The capacitive coupling fractions with readout strip and floating strip incidences were studied using the beam test data and SPICE simulation.**

***Index Terms*—Silicon microstrip detectors, Capacitive coupling, Capacitance**

I. Introduction

THE High Energy Cosmic Radiation Detection (HERD) facility is a dedicated particle and astrophysical experiment for the Chinese space station. It aims to achieve several key scientific objectives, including indirect searches for dark matter, precise spectroscopy, and composition measurements of cosmic rays, and monitoring high-energy gamma rays [1]. One of the unresolved phenomena in cosmic ray detection is the "knee", which refers to the steepening of primary cosmic rays near the PeV energy range [2]. The operation of HERD is expected to make significant contributions to understanding this phenomenon.

The HERD facility comprises a 3-D cubic imaging calorimeter (CALO) surrounded by five sides of trackers, Plastic Scintillator Detector (PSD) and Silicon Charge Detector (SCD) [3]. The envelope size of the HERD facility is 3.0 × 2.3 × 1.7 m^3. SCD is located at the outmost of HERD, as shown in Fig. 1.

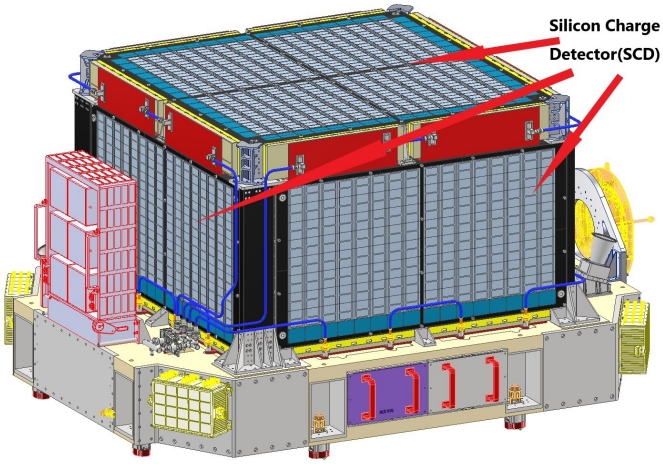

Fig. 1. Schematics of the HERD detector.

The SCD is designed to measure the charge of high-energy cosmic ray nuclei ranging from Z of 1 to about 28. The SCD is composed of a Top-SCD unit covering an area of 1.8 × 1.8 m^2, and four Side-SCD units with an area of 1.6 × 1.1 m^2 each. Each SCD unit consists of eight layers of single-sided silicon microstrip detectors. The adjacent layers are installed in orthogonal directions to identify the charge and trajectories of incoming charged particles [4].

A silicon microstrip detector can be modeled as a network of capacitors, which includes the bulk capacitors, the interstrip capacitors, and the coupling capacitors [5,6]. When a charge signal is generated within a strip that has been hit, it can be capacitively coupled to neighboring strips through the capacitor network. This capacitive coupling effect is negligible when the coupling capacitance is significantly larger than the interstrip capacitance. On the contrary, this capacitive coupling effect can be enhanced by using smaller coupling capacitors as discussed in this paper.

The electronic design of SCD is inherited from the Silicon Tungsten Tracker of the Dark Matter Explorer (DAMPE), whose linear dynamic range can only directly measure the signal of Z = 1 ∼ 6. The SCD is proposed to increase the dynamic range to measure the signal of Z = 1 ∼ 28 by enhancing the capacitive coupling effect. The small signals from low-Z particles can be easily measured using the fired

This research is supported by the States Key Project of Research and Development Plan (2021YFA0718403, 2021YFA0718404, 2022YFF0503302), the National Natural Science Foundation of China (Projects: 12061131007).

Ruo-Si Lu, Rui Qiao, Ke Gong, Wen-Xi Peng, Wei-Shuai Zhang, Dong-Ya Guo, Qi Wu, Peng Hu, Xuan Liu, Bing Lu and Yi-Rong Zhang are with the Institute of High Energy Physics, Chinese Academy of Sciences, Beijing 100049, China (e-mail: lurs@ihep.ac.cn; qiaorui@ihep.ac.cn; gongk@ihep.ac.cn; pengwx@ihep.ac.cn; zhangws@ihep.ac.cn; guody@ihep.ac.cn; wuqi98@ihep.ac.cn; hupeng@ihep.ac.cn; liuxuan@ihep.ac.cn; lubing@ihep.ac.cn; 2021226055026@stu.scu.edu.cn).

Ruo-Si Lu, Rui Qiao, Ke Gong, Wen-Xi Peng and Qi Wu are with the University of Chinese Academy of Sciences, Beijing 100049, China (e-mail: lurs@ihep.ac.cn; qiaorui@ihep.ac.cn; gongk@ihep.ac.cn; pengwx@ihep.ac.cn; wuqi98@ihep.ac.cn).

Jia-Ju Wei, Yi-Ming Hu, and Jian-Hua Guo are with the Key Laboratory of Dark Matter and Space Astronomy, Purple Mountain Observatory, Chinese Academy of Sciences, Nanjing 210008, China (e-mail: weijj@pmo.ac.cn; huyiming@pmo.ac.cn; jhguo@pmo.ac.cn).

Jian-Hua Guo is with School of Astronomy and Space Science, University of Science and Technology of China, Hefei 230026, China (e-mail: jhguo@pmo.ac.cn).

Wei-Shuai Zhang is with School of Physics and Astronomy, China West Normal University, Nanchong 637002, China (e-mail: zhangws@ihep.ac.cn).

Xuan Liu is with North China University of Technology, Beijing, 100144, China (e-mail: liuxuan@ihep.ac.cn).

Yi-Rong Zhang is with Sichuan University, Chengdu, 610065, China (e-mail: 2021226055026@stu.scu.edu.cn).

Waveform Simulation for Scintillation Characteristics of NaI(Tl) Crystal

J.J. Choi[a], C. Ha[b], E.J. Jeon[c], K.W. Kim[c], S.K. Kim[a], Y.D. Kim[c,d], Y.J. Ko[c], B.C. Koh[b], H.S. Lee[c,d], S.H. Lee[d,c], S.M. Lee[a], B.J. Park[d,c], G.H Yu[e,c]

[a]*Department of Physics and Astronomy, Seoul National University, Seoul 08826, Republic of Korea*
[b]*Department of Physics, Chung-Ang University, Seoul 06973, Republic of Korea*
[c]*Center for Underground Physics, Institute for Basic Science (IBS), Daejeon 34126, Republic of Korea*
[d]*IBS School, University of Science and Technology (UST), Daejeon 34113, Republic of Korea*
[e]*Department of Physics, Sungkyunkwan University, Suwon 16419, Republic of Korea*

Abstract

The lowering of the energy threshold in the NaI detector is crucial not only for comprehensive validation of DAMA/LIBRA but also for exploring new possibilities in the search for low-mass dark matter and observing coherent elastic scattering between neutrino and nucleus. Alongside hardware enhancements, extensive efforts have focused on refining event selection to discern noise, achieved through parameter development and the application of machine learning. Acquiring pure, unbiased datasets is crucial in this endeavor, for which a waveform simulation was developed. The simulation data were compared with the experimental data using several pulse shape discrimination parameters to test its performance in describing the experimental data. Additionally, we present the outcomes of multi-variable machine learning trained with simulation data as a scintillation signal sample. The distributions of outcomes for experimental and simulation data show a good agreement. As an application of the waveform simulation, we validate the trigger efficiency alongside estimations derived from the minimally biased measurement data.

Email addresses: kwkim@ibs.re.kr (K.W. Kim), yjko@ibs.re.kr (Y.J. Ko)

Fabrication of ^{108}Cd target for the astrophysical p-process studies

Sukhendu Saha[a,b], Mousri Paul[a,b], Lalit Kumar Sahoo[a,b], Dipali Basak[a,b], Tanmoy Bar[a,b], Jagannath Datta[c], Sandipan Dasgupta[c], G.L.N. Reddy[d], Chinmay Basu[a]

[a]*Nuclear Physics Division, Saha Institute of Nuclear Physics, 1/AF Bidhannagar, Saltlake, Kolkata-700064, India*
[b]*Homi Bhabha National Institute, Anushaktinagar, Mumbai-400094, India*
[c]*Analytical Chemistry Division, Bhabha Atomic Research Centre, Variable Energy Cyclotron Centre, 1/AF Bidhannagar, Saltlake, Kolkata-700064, India*
[d]*National Centre for Compositional Characterization of Materials, BARC, ECIL Post, Hyderabad-500062, India*

Abstract

The detailed process of preparing enriched ^{108}Cd targets on mylar and copper backing using the vacuum evaporation technique is described. These targets were employed in an experiment to measure the proton capture cross-section at energies significantly below the Coulomb barrier, for the astrophysical p-process studies [1][2]. Due to the low melting point and high vapor pressure of cadmium, some adjustments were implemented in the Telemark multipocket e-beam setup. The target thickness was determined through the measurement of alpha particle energy loss from a triple alpha source and also by RBS measurements. The thickness of the ^{108}Cd films varies between 290 to 660 μg/cm^2, with a non-uniformity of approximately 10%. X-ray Photoelectron Spectroscopy (XPS) and X-ray Fluorescence (XRF) analyses were conducted to examine the presence of impurities and to assess surface morphology, phase, and chemical composition.

Keywords:
p-nuclei, vacuum evaporation, RBS, XPS, XRF

Prepared for submission to JHEP

Cluster Scanning: a novel approach to resonance searches

I. Oleksiyuk,[a,b] **J. A. Raine,**[a] **M. Krämer,**[c] **S. Voloshynovskiy,**[b] **T. Golling**[a]

[a] *Département de Physique Nucléaire et Corpusculaire, University of Geneva, 1211 Geneva, Switzerland*

[b] *Centre Universitaire d'Informatique, University of Geneva, 1211 Geneva, Switzerland*

[c] *Institute for Theoretical Particle Physics and Cosmology, RWTH Aachen University, 52074 Aachen, Germany*

E-mail: ivan.oleksiyuk@unige.ch, john.raine@unige.ch, mkraemer@physik.rwth-aachen.de, svyatoslav.voloshynovskyy@unige.ch, tobias.golling@unige.ch

Abstract: We propose a new model-independent method for new physics searches called Cluster Scanning. It uses the k-means algorithm to perform clustering in the space of low-level event or jet observables, and separates potentially anomalous clusters to construct a signal-enriched region. The invariant mass spectra in these two regions are then used to determine whether a resonant signal is present. A pseudo-analysis on the LHC Olympics dataset with a Z' resonance shows that Cluster Scanning outperforms the widely used 4-parameter functional background fitting procedures, reducing the number of signal events needed to reach a 3σ significant access by a factor of 0.61. Emphasis is placed on the speed of the method, which allows the test statistic to be calibrated on synthetic data.

T-odd gluon distribution functions in a spectator model

Alessandro Bacchetta,[1,2,*] Francesco Giovanni Celiberto,[3,†] and Marco Radici[2,‡]

[1] *Dipartimento di Fisica, Università di Pavia, via Bassi 6, I-27100 Pavia*
[2] *INFN Sezione di Pavia, via Bassi 6, I-27100 Pavia, Italy*
[3] *Universidad de Alcalá (UAH), Departamento de Física y Matemáticas, E-28805 Alcalá de Henares, Madrid, Spain*

(Dated: Wednesday 28th February, 2024, 03:00)

We present a model calculation of T-odd transverse-momentum-dependent distributions of gluons in the nucleon. The model is based on the assumption that a nucleon can emit a gluon, and what remains after the emission is treated as a single spectator particle. This spectator particle is considered to be on-shell, but its mass is allowed to take a continuous range of values, described by a spectral function. The final-state interaction that is necessary to generate T-odd functions is modeled as the exchange of a single gluon between the spectator and the outgoing parton.

PACS numbers: 12.38.-t, 12.40.-y, 14.70.Dj

CONTENTS

* alessandro.bacchetta@unipv.it
† francesco.celiberto@uah.es
‡ marco.radici@pv.infn.it

Preprint — Submitted to Computing and Software for Big Science

A case study of sending graph neural networks back to the test bench for applications in high-energy particle physics

Emanuel Pfeffer · **Michael Waßmer** · **Yee-Ying Cung** · **Roger Wolf** · **Ulrich Husemann**

Abstract In high-energy particle collisions, the primary collision products usually decay further resulting in tree-like, hierarchical structures with a priori unknown multiplicity. At the stable-particle level all decay products of a collision form permutation invariant sets of final state objects. The analogy to mathematical graphs gives rise to the idea that graph neural networks (GNNs), which naturally resemble these properties, should be best-suited to address many tasks related to high-energy particle physics. In this paper we describe a benchmark test of a typical GNN against neural networks of the well-established deep fully-connected feed-forward architecture. We aim at performing this comparison maximally unbiased in terms of nodes, hidden layers, or trainable parameters of the neural networks under study. As physics case we use the classification of the final state X produced in association with top quark-antiquark pairs in proton-proton collisions at the Large Hadron Collider at CERN, where X stands for a bottom quark-antiquark pair produced either non-resonantly or through the decay of an intermediately produced Z or Higgs boson.

Keywords Graph Neural Networks · Deep Neural Networks · High-Energy Particle Physics · LHC

Emanuel Pfeffer[1] (corresponding author)
E-mail: emanuel.pfeffer@kit.edu

Michael Waßmer[1]
E-mail: michael.wassmer@kit.edu

Yee-Ying Cung
E-mail: yeeying.cung@web.de

Roger Wolf[1]
E-mail: roger.wolf@kit.edu

Ulrich Husemann[1]
E-mail: ulrich.husemann@kit.edu

[1] Karlsruhe Institute of Technology, Institute of Experimental Particle Physics, Karlsruhe, Germany

Eur. Phys. J. C manuscript No.
(will be inserted by the editor)

ZU-TH 12/24, KA-TP-03-2024, P3H-24-011

A comparative study of flavour-sensitive observables in hadronic Higgs decays

Benjamin Campillo Aveleira[a,1,2], **Aude Gehrmann–De Ridder**[b,1,3], **Christian T Preuss**[c,1,4]

[1]Institute for Theoretical Physics, ETH, 8093 Zürich, Switzerland
[2]Institute for Theoretical Physics, KIT, 76131 Karlsruhe, Germany
[3]Department of Physics, University of Zürich, 8057 Zürich, Switzerland
[4]Department of Physics, University of Wuppertal, 42119 Wuppertal, Germany

Received: date / Accepted: date

Abstract Jet production from hadronic Higgs decays at future lepton colliders will have significantly different phenomenological implications than jet production via off-shell photon and Z-boson decays, owing to the fact that Higgs bosons decay to both pairs of quarks and gluons. We compute observables involving flavoured jets in hadronic Higgs decays to three partons at Born level including next-to-leading order corrections in QCD (i.e up to $\mathcal{O}(\alpha_s^2)$). The calculation is performed in the framework of an effective theory in which the Higgs boson couples directly to gluons and massless b-quarks retaining a non-vanishing Yukawa coupling. For the following flavour sensitive observables: the energy of the leading and subleading flavoured jet, the angular separation and the invariant mass of the leading b-$\bar{b}$ pair, we contrast the results obtained in both Higgs decay categories and using either of the infrared-safe flavoured jet algorithms flavour-k_T and flavour-dressing.

Keywords flavoured jets · hadronic Higgs decays · NLO QCD

1 Introduction

Precision studies of the Higgs boson discovered at LHC by CMS and ATLAS [1,2] will become possible at future lepton colliders such as [3,4], all aiming to operate as Higgs factories. In this clean experimental environment, where interactions take place at well-defined centre-of mass energies, it is expected to enable model-independent measurements of the Higgs couplings to gauge bosons and fermions at the level of a few percent. At these future lepton colliders, in particular it will become possible to have access to so-far unobserved hadronic decay channels such as Higgs decays to gluons. The latter is currently inaccessible in hadron-collider environments due to the presence of overwhelming QCD backgrounds. Only the $H \to b\bar{b}$ decay was observed to date [5,6] in associated vector-boson production where the leptonic decay signature of the vector boson helps to identify the $H \to b\bar{b}$ decay.

Hadronic Higgs decays to at least two final state hard partons proceed via two main decay modes; either as Yukawa-induced decay to a bottom-quark pair, $H \to b\bar{b}$, or as a heavy-quark-loop induced decay to two gluons, $H \to gg$. In the latter category, observables are computed in the framework of an effective field theory, in which the top-quark loop is integrated out into an effective point-like Hgg vertex.

So far these two categories of Higgs decay processes have been considered together in the computation of flavour-agnostic event-shape observables, i.e., for three-jet-like final states in [7,8,9,10,11] and for four jet-like final states in [12]. It was also recently suggested to determine branching ratios in hadronic Higgs decays via fractional energy correlators [13]. Flavour-sensitive jet observables related to the presence of a flavoured jet in the final state have so far been computed for the following LHC processes: VH production, with $H \to b\bar{b}$ or $Z + b$-jet and $Z/W + c$-jet, with the vector boson decaying leptonicallly in all cases. More precisely, parton-level predictions including up to NNLO QCD corrections using massless charm or bottom quarks at the origin of the flavoured jet have been computed most re-

[a]e-mail: benjamin.campillo@kit.edu
[b]e-mail: gehra@phys.ethz.ch
[c]e-mail: preuss@uni-wuppertal.de

Impact of strong magnetic field, baryon chemical potential, and medium anisotropy on polarization and spin alignment of hadrons

Bhagyarathi Sahoo,* Captain R. Singh,† and Raghunath Sahoo‡
Department of Physics, Indian Institute of Technology Indore, Simrol, Indore 453552, India
(Dated: February 28, 2024)

The recent observation of global polarization of Λ ($\bar{\Lambda}$) hyperons and spin alignment of ϕ and K^{*0} vector mesons create remarkable interest in investigating the particle polarization in the relativistic fluid produced in heavy-ion collisions at GeV/TeV energies. Among other sources of polarization, the Debye mass of a medium plays a crucial role in particle polarization. Any modification brought to the effective mass due to the temperature, strong magnetic field (eB), baryonic chemical potential (μ_B), and medium anisotropy (ξ), vorticity, etc., certainly affects the particle polarization. In this work, we explore the global hyperon polarization and the spin alignment of vector mesons corresponding to the strong magnetic field, baryonic chemical potential, and medium anisotropy. We find that the degree of polarization is flavor-dependent for hyperons. Meanwhile, vector meson spin alignment depends on the hadronization mechanisms of initially polarized quarks and anti-quarks. Medium anisotropy significantly changes the degree of polarization in comparison with the magnetic field and baryon chemical potential.

I. INTRODUCTION

So far, the thermalized state of strongly interacting partons, called quark-gluon plasma (QGP), is probed in heavy-ion collisions through a baseline, the *pp* collisions. It was assumed that QGP existence in *pp* collisions is next to impossible because it lacks the necessary conditions for QGP to be formed. On the contrary, in recent LHC events, ultra- relativistic *pp* collision experiments have reported behavior similar to heavy-ion collisions, e.g., collective flow, strangeness enhancement, etc [1, 2]. However, other studies suggest similar phenomena may arise due to the other QCD processes [3**?** , 4]. These studies raise a question concerning the present QGP signatures and a need for the next generation of probes. In the quest for such a baseline-independent probe, polarization comes into picture and can have implications for understanding hot QCD matter. The particle production mechanisms lead to a finite polarization of the light/heavy baryons and vector mesons [5]. However, there are various sources by which hadrons can get polarized in ultra-relativistic collisions. One such primary source could be the initial state polarization, which arises due to the motion and spin of the constituent quarks of the colliding nucleons. This initial state polarization can be transmitted to the quarks participating in the collision process. The magnetic field produced by the charged spectator protons in such collisions interacts with the electric charge and spin of the quarks, which may lead to quark polarization. A topological charge imbalance in the presence of an external magnetic field leads to the charge separation in the direction of the magnetic field. This phenomenon is known as the chiral magnetic effect (CME) [6, 7]. If QGP exhibits chiral symmetry restoration, then CME could lead to quark polarization along the direction of the magnetic field. A similar phenomenon called chiral vortical effect (CVE) is expected due to the non-zero local vorticity, which also contributes to the hadron polarization [8, 9]. The hydrodynamic behavior or collective motion of QGP can also induce polarization in the quark distribution due to the anisotropic expansion [10, 11]. Determining the precise sources and types of polarization in ultra-relativistic collisions requires sophisticated theoretical studies with corresponding experimental observations.

In 2005, Liang and Wang predicted in non-central heavy-ion collisions, the orbital angular momentum (OAM) of the partonic system polarizes the quarks and anti-quarks through spin-orbit coupling. They asserted that the initial partons created in the collisions could generate a longitudinal fluid shear distribution representing the local relative OAM in the same direction as global OAM at a finite impact parameter. This quark polarization manifests the polarization of the hadrons (with finite spin) along the direction of OAM during the process of hadronization [12–15]. Apart from global polarization of hadrons, such global quark polarization has many observable consequences, such as left-right asymmetry in hadron spectra and global transverse polarization of thermal photons, dileptons, etc. [16, 17]. They have studied the global polarization of hyperons [12] and spin alignment of vector mesons [13] in different hadronization scenarios. Following, in 2013, Becattini et al. predicted the global spin polarization of Λ hyperons due to the OAM-manifested thermal vorticity [18]. Various theoretical predictions of global Λ hyperons polarization by different hydrodynamic and transport models are well agreed with the experimental results available at Relativistic Heavy Ion Collider (RHIC) [19–27]. These hydrodynamic and transport

* Bhagyarathi.Sahoo@cern.ch
† captainriturajsingh@gmail.com
‡ Raghunath.Sahoo@cern.ch (Corresponding Author)

Prepared for submission to JHEP

Constraining Asymmetric Dark Matter using Colliders and Direct Detection

Arnab Roy [a,b], **Basudeb Dasgupta** [a] and **Monoranjan Guchait** [a]

[a] *Tata Institute of Fundamental Research, Homi Bhabha Road, Colaba, Mumbai 400005, India*
[b] *School of Physics and Astronomy, Monash University, Wellington Road, Clayton, Victoria 3800, Australia*

E-mail: arnab.roy1@monash.edu, bdasgupta@theory.tifr.res.in, guchait@tifr.res.in

Abstract: We reappraise the viability of asymmetric dark matter (ADM) realized as a Dirac fermion coupling dominantly to the Standard Model fermions. Treating the interactions of such a DM particle with quarks/leptons in an effective-interactions framework, we derive updated constraints using mono-jet searches from the Large Hadron Collider (LHC) and mono-photon searches at the Large Electron-Positron (LEP) collider. We carefully model the detectors used in these experiments, which is found to have significant impact. The constraint of efficient annihilation of the symmetric part of the ADM, as well as other observational constraints are synthesized to produce a global picture. Consistent with previous work, we find that ADM with mass in the range 1–100 GeV is strongly constrained, thus ruling out its best motivated mass range. However, we find that leptophilic ADM remains allowed for $\gtrsim 10$ GeV DM, including bounds from colliders, direct detection, and stellar heating. We forecast that the Future Circular Collider for electron-positron collisions (FCC-ee) will improve sensitivity to DM-lepton interactions by almost an order of magnitude.

Direct Detection of Dark Photon Dark Matter with the James Webb Space Telescope

Haipeng An,[1,2,3,4,*] Shuailiang Ge,[3,5,†] Jia Liu,[5,3,‡] and Zhiyao Lu[5,§]

[1]*Department of Physics, Tsinghua University, Beijing 100084, China*

[2]*Center for High Energy Physics, Tsinghua University, Beijing 100084, China*

[3]*Center for High Energy Physics, Peking University, Beijing 100871, China*

[4]*Frontier Science Center for Quantum Information, Beijing 100084, China*

[5]*School of Physics and State Key Laboratory of Nuclear Physics and Technology, Peking University, Beijing 100871, China*

(Dated: February 28, 2024)

Abstract

In this study, we propose an investigation into dark photon dark matter (DPDM) within the infrared frequency band, utilizing highly sensitive infrared light detectors commonly integrated into space telescopes, such as the James Webb Space Telescope (JWST). The presence of DPDM induces electron oscillations in the reflector of these detectors. Consequently, these oscillating electrons can emit monochromatic electromagnetic waves with a frequency almost equivalent to the mass of DPDM. By employing the stationary phase approximation, we can demonstrate that when the size of the reflector significantly exceeds the wavelength of the electromagnetic wave, the contribution to the electromagnetic wave field at a given position primarily stems from the surface unit perpendicular to the relative position vector. This simplification results in the reduction of electromagnetic wave calculations to ray optics. By applying this concept to JWST, our analysis of observational data demonstrates the potential to establish constraints on the kinetic mixing between the photon and dark photon within the range [10, 500] THz. Despite JWST not being optimized for DPDM searches, our findings reveal constraints comparable to those obtained from the XENON1T experiment in the laboratory, as well as astrophysical constraints from solar emission. Additionally, we explore strategies to optimize future experiments specifically designed for DPDM searches.

* anhp@mail.tsinghua.edu.cn

† sge@pku.edu.cn

‡ jialiu@pku.edu.cn

§ 2000011457@stu.pku.edu.cn

PROCEEDINGS OF SCIENCE

Theoretical Highlights of CP Violation in B Decays

Eleftheria Malami[a,b,*]

[a] *Center for Particle Physics Siegen (CPPS), Theoretische Physik 1, Universität Siegen, D-57068 Siegen, Germany*

[b] *Nikhef, Science Park 105, 1098 XG Amsterdam, Netherlands*

E-mail: Eleftheria.Malami@uni-siegen.de, emalami@nikhef.nl

In this presentation, we discuss recent key topics in theoretical analyses of CP violation in benchmarks decays of the B meson. We provide the most updated values of the mixing phases and discuss the importance of including the penguin contributions in their studies. Exploring intriguing patterns in purely tree decays, interesting new methodologies can be developed and applied. New data related to the CP asymmetries of key modes like $B_d^0 \to \pi^0 K_S$ and $B_s^0 \to K^+K^-$ lead to interesting results. The new $R_{K^{(*)}}$ measurement, compatible with the Standard Model, can still allow for electron-muon symmetry violation through new sources of CP violation.

16th International Conference on Heavy Quarks and Leptons (HQL2023)
28 November-2 December 2023
TIFR, Mumbai, Maharashtra, India

*Speaker

https://pos.sissa.it/

allows us to study these anomalies and search for hints of NP is discussed in Refs. [14, 15]. Let us summarise the key points of this methodology.

As a first step, we explore CP violation. Due to B_q^0–$\bar{B}_q^0$ mixing, interference effects arise between the $\bar{B}_s^0 \to D_s^+K^-$ and $B_s^0 \to D_s^+K^-$ channels. These interference effects lead to a time-dependent CP asymmetry, which yields the observables C, S, $\mathcal{A}_{\Delta\Gamma}$ and their CP conjugates. A measure of the strength of the interference effects is given by the quantities ξ and $\bar{\xi}$. Therefore, one can use the observables C, S, $\mathcal{A}_{\Delta\Gamma}$ and $\bar{C}$, $\bar{S}$, $\bar{\mathcal{A}}_{\Delta\Gamma}$, in order to determine ξ and $\bar{\xi}$, respectively, from the experimental data in an unambiguous way. Within the SM, in the product $\xi \times \bar{\xi}$ hadronic matrix elements cancel out allowing a theoretically clean extraction to $(\phi_s + \gamma)$. In the presence of NP, the generalisation of this relation takes the following form:

$$\xi \times \bar{\xi} = \sqrt{1 - 2\left[\frac{C + \bar{C}}{(1+C)\left(1+\bar{C}\right)}\right]} e^{-i[2(\phi_s + \gamma_{\rm eff})]}, \tag{6}$$

where again hadronic uncertainties cancel. In particular, here it is possible that $C + \bar{C}$ is not equal to 0, as in the SM. The above expression leads to a theoretically clean determination of the angle:

$$\gamma_{\rm eff} \equiv \gamma + \gamma_{\rm NP}, \tag{7}$$

where $\gamma_{\rm NP}$ is a function of the NP parameters ρ, φ, δ, and $\bar{\rho}$, $\bar{\varphi}$, $\bar{\delta}$ (for the CP conjugate case). Here, $\rho = \left[A(\bar{B}_s^0 \to D_s^+K^-)_{\rm NP}/A(\bar{B}_s^0 \to D_s^+K^-)_{\rm SM}\right]$ measures the strength of NP, while δ and φ denote the CP-conserving and CP-violating phases, and similarly for $\bar{\rho}$, $\bar{\varphi}$, $\bar{\delta}$. Using information on γ [16] from other processes, we extract $\gamma_{\rm NP}$.

The second step corresponds to information from the branching ratios. We create ratios by combining the branching fractions of the non-leptonic decays we study with differential branching ratios of their semi-leptonic partner channels. These ratios with the semileptonic decays minimize the dependence on the CKM matrix elements and the hadronic form factors. Therefore, they provide a useful setup which permits the extraction of the colour factors $|a_1|$ from the data in the theoretically cleanest possible manner. Comparing these experimental results with theoretical predictions, we find tensions even up to the 4.8 σ level. This intriguing pattern is in line with what we expect from the puzzling situation with γ. In order to interpret these $|a_1|$ deviations, we introduce the quantities:

$$\bar{b} \equiv \frac{\langle \mathcal{B}(\bar{B}_s^0 \to D_s^+K^-)_{\rm th}\rangle}{\mathcal{B}(\bar{B}_s^0 \to D_s^+K^-)_{\rm th}^{\rm SM}} = 1 + 2\,\bar{\rho}\cos\bar{\delta}\cos\bar{\varphi} + \bar{\rho}^2, \tag{8}$$

$$b \equiv \frac{\langle \mathcal{B}(B_s^0 \to D_s^-K^+)_{\rm th}\rangle}{\mathcal{B}(B_s^0 \to D_s^-K^+)_{\rm th}^{\rm SM}} = 1 + 2\,\rho\cos\delta\cos\varphi + \rho^2, \tag{9}$$

where now we use as input the theoretical expectation of $|a_1|$. The extracted values of b and $\bar{b}$ deviate from the SM. We highlight that making use of other control channels, we are able to constrain the contributions from exchange diagrams and no anomalous enhancement is observed due to these topologies.

Last but not least, we explore how much room there is for NP utilising all three $\gamma_{\rm eff}$, b and $\bar{b}$. More specifically, we obtain correlations between the NP parameters $\rho(\varphi)$ and $\bar{\rho}(\bar{\varphi})$, assuming that the strong phases equal to 0. Constraining these NP parameters, we find that it is possible to accommodate the current data with new contributions of moderate size.

The symmetry approach to quark and lepton masses and mixing

Gui-Jun Ding[a] *, José W.F. Valle[b] †

[a] *Department of Modern Physics, University of Science and Technology of China, Hefei, Anhui 230026, China*

[b] *AHEP Group, Instituto de Física Corpuscular - CSIC/Universitat de València, Parque Científico C/Catedratico José Beltrán, 2, E-46980 Paterna (València) - SPAIN*

Abstract

The Standard Model lacks an organizing principle to describe quark and lepton "flavours". We review the impact of neutrino oscillation experiments, which show that leptons mix very differently from quarks, placing a major challenge, but also providing a key input to the flavour puzzle. We briefly sketch the seesaw and "scotogenic" approaches to neutrino mass, the latter including also WIMP dark matter. We discuss the limitations of popular neutrino mixing patterns and examine the possibility that they arise from symmetry, giving a bottom-up approach to residual flavour and CP symmetries. We show how family and/or CP symmetries can generate novel viable and predictive mixing patterns. We review the model-independent ways to predict lepton mixing and test both mixing predictions as well as mass sum rules. We also discuss UV-complete flavour theories in four and more space-time dimensions, and their predictions. Benchmarks given include an A_4 scotogenic construction with trimaximal mixing pattern TM2. Higher-dimensional completions are also reviewed, such as 5-D warped flavordynamics. We present a T' warped flavordynamics theory with TM1 mixing pattern, detectable neutrinoless double beta decay rates and providing a very good fit of flavour observables, including quarks. We also review how 6-D orbifolds offer a way to determine the structure of the 4-D family symmetry from the symmetries between the extra-D branes. We describe a scotogenic A_4 orbifold predicting the "golden" quark-lepton mass relation, large neutrino mass with normal ordering, higher atmospheric octant, restricted reactor angle, and an excellent global flavour fit, including quark observables. Finally, we discuss promising recent progress in tackling the flavor issue through the use of modular symmetries.

Keywords: Fermion mixing, CP violation, generalized CP, flavor and modular symmetry, orbifolds, warped-flavordynamics.

*E-mail: dinggj@ustc.edu.cn

†E-mail: valle@ific.uv.es

Exploring the sensitivity to non-standard and generalized neutrino interactions through coherent elastic neutrino-nucleus scattering with a NaI detector

Sabya Sachi Chatterjee,[1,2,*] Stéphane Lavignac,[2,†] O. G. Miranda,[3,‡] and G. Sanchez Garcia[4,§]

[1] *Institut für Astroteilchenphysik, Karlsruher Institut für Technologie (KIT), 76131 Karlsruhe, Germany*

[2] *Institut de Physique Théorique, Université Paris Saclay, CNRS, CEA, F-91191 Gif-sur-Yvette, France*

[3] *Departamento de Física, Centro de Investigación y de Estudios Avanzados del IPN, Apartado Postal 14-740 07000, Ciudad de Mexico, Mexico*

[4] *Instituto de Física Corpuscular (CSIC-Universitat de València), Parc Científic UV, C/ Catedràtico José Beltrán, 2, 46980 Paterna, Spain*

After the first observation of coherent elastic neutrino-nucleus scattering (CEνNS) by the COHERENT collaboration, many efforts are being made to improve the measurement of this process, making it possible to constrain new physics in the neutrino sector. In this paper, we study the sensitivity to non-standard interactions (NSIs) and generalized neutrino interactions (GNIs) of a NaI detector with characteristics similar to the one that is currently being deployed at the Spallation Neutron Source at Oak Ridge National Laboratory. We show that such a detector, whose target nuclei have significantly different proton to neutron ratios (at variance with the current CsI detector), could help to partially break the parameter degeneracies arising from the interference between the Standard Model and NSI contributions to the CEνNS cross section, as well as between different NSI parameters. By contrast, only a slight improvement over the current CsI constraints is expected for parameters that do not interfere with the SM contribution. We find that a significant reduction of the background level would make the NaI detector considered in this paper very efficient at breaking degeneracies among NSI parameters.

I. INTRODUCTION

Coherent elastic neutrino-nucleus scattering (CEνNS) [1] is a privileged process to probe new physics in the neutrino sector. So far, the only measurements of CEνNS have been done at the Spallation Neutron Source (SNS) at Oak Ridge National Laboratory, USA, by the COHERENT collaboration. The first observation of this process was performed with a CsI detector [2, 3]. Another detector, with liquid Argon as a target, was subsequently used by the COHERENT collaboration [4].

* sabya.chatterjee@kit.edu
† stephane.lavignac@ipht.fr
‡ omar.miranda@cinvestav.mx
§ gsanchez@fis.cinvestav.mx

EUROPEAN ORGANIZATION FOR NUCLEAR RESEARCH (CERN)

CERN-EP-2024-038
2024/02/28

CMS-BPH-23-002

Observation of the $\Xi_b^- \to \psi(2S)\Xi^-$ decay and studies of the Ξ_b^{*0} baryon in proton-proton collisions at $\sqrt{s} = 13\,\text{TeV}$

The CMS Collaboration*

Abstract

The first observation of the decay $\Xi_b^- \to \psi(2S)\Xi^-$ and measurement of the branching ratio of $\Xi_b^- \to \psi(2S)\Xi^-$ to $\Xi_b^- \to J/\psi\Xi^-$ are presented. The J/ψ and $\psi(2S)$ mesons are reconstructed using their dimuon decay modes. The results are based on proton-proton colliding beam data from the LHC collected by the CMS experiment at $\sqrt{s} = 13\,\text{TeV}$ in 2016–2018, corresponding to an integrated luminosity of $140\,\text{fb}^{-1}$. The branching fraction ratio is measured to be $\mathcal{B}(\Xi_b^- \to \psi(2S)\Xi^-)/\mathcal{B}(\Xi_b^- \to J/\psi\Xi^-) = 0.84^{+0.21}_{-0.19}\,(\text{stat}) \pm 0.10\,(\text{syst}) \pm 0.02\,(\mathcal{B})$, where the last uncertainty comes from the uncertainties in the branching fractions of the charmonium states. New measurements of the Ξ_b^{*0} baryon mass and natural width are also presented, using the $\Xi_b^-\pi^+$ final state, where the Ξ_b^- baryon is reconstructed through the decays $J/\psi\Xi^-$, $\psi(2S)\Xi^-$, $J/\psi\Lambda K^-$, and $J/\psi\Sigma^0 K^-$. Finally, the fraction of the Ξ_b^- baryons produced from Ξ_b^{*0} decays is determined.

Submitted to Physical Review D

*See Appendix A for the list of collaboration members

Belle II Preprint 2024-006
KEK Preprint 2023-53

A new graph-neural-network flavor tagger for Belle II and measurement of $\sin 2\phi_1$ in $B^0 \to J/\psi K^0_S$ decays

I. Adachi, L. Aggarwal, H. Ahmed, H. Aihara, N. Akopov, A. Aloisio, N. Anh Ky, D. M. Asner, H. Atmacan, T. Aushev, V. Aushev, M. Aversano, R. Ayad, V. Babu, H. Bae, S. Bahinipati, P. Bambade, Sw. Banerjee, S. Bansal, M. Barrett, J. Baudot, A. Baur, A. Beaubien, F. Becherer, J. Becker, J. V. Bennett, F. U. Bernlochner, V. Bertacchi, M. Bertemes, E. Bertholet, M. Bessner, S. Bettarini, B. Bhuyan, F. Bianchi, L. Bierwirth, T. Bilka, S. Bilokin, D. Biswas, A. Bobrov, D. Bodrov, A. Bolz, A. Bondar, A. Bozek, M. Bračko, P. Branchini, R. A. Briere, T. E. Browder, A. Budano, S. Bussino, M. Campajola, L. Cao, G. Casarosa, C. Cecchi, J. Cerasoli, M.-C. Chang, P. Chang, P. Cheema, C. Chen, B. G. Cheon, K. Chilikin, K. Chirapatpimol, H.-E. Cho, K. Cho, S.-J. Cho, S.-K. Choi, S. Choudhury, J. Cochran, L. Corona, S. Das, F. Dattola, E. De La Cruz-Burelo, S. A. De La Motte, G. De Nardo, M. De Nuccio, G. De Pietro, R. de Sangro, M. Destefanis, S. Dey, R. Dhamija, A. Di Canto, F. Di Capua, Z. Doležal, T. V. Dong, M. Dorigo, K. Dort, D. Dossett, S. Dreyer, S. Dubey, G. Dujany, P. Ecker, M. Eliachevitch, P. Feichtinger, T. Ferber, D. Ferlewicz, T. Fillinger, C. Finck, G. Finocchiaro, A. Fodor, F. Forti, A. Frey, B. G. Fulsom, A. Gabrielli, E. Ganiev, M. Garcia-Hernandez, R. Garg, G. Gaudino, V. Gaur, A. Gaz, A. Gellrich, G. Ghevondyan, D. Ghosh, H. Ghumaryan, G. Giakoustidis, R. Giordano, A. Giri, A. Glazov, B. Gobbo, R. Godang, O. Gogota, P. Goldenzweig, W. Gradl, T. Grammatico, E. Graziani, D. Greenwald, Z. Gruberová, T. Gu, Y. Guan, K. Gudkova, Y. Han, K. Hara, T. Hara, K. Hayasaka, H. Hayashii, S. Hazra, C. Hearty, M. T. Hedges, A. Heidelbach, I. Heredia de la Cruz, M. Hernández Villanueva, T. Higuchi, M. Hoek, M. Hohmann, P. Horak, C.-L. Hsu, T. Humair, T. Iijima, K. Inami, N. Ipsita, A. Ishikawa, R. Itoh, M. Iwasaki, P. Jackson, W. W. Jacobs, D. E. Jaffe, E.-J. Jang, Q. P. Ji, S. Jia, Y. Jin, K. K. Joo, H. Junkerkalefeld, H. Kakuno, D. Kalita, A. B. Kaliyar, J. Kandra, K. H. Kang, S. Kang, G. Karyan, T. Kawasaki, F. Keil, C. Kiesling, C.-H. Kim, D. Y. Kim, K.-H. Kim, Y.-K. Kim, H. Kindo, K. Kinoshita, P. Kodyš, T. Koga, S. Kohani, K. Kojima, A. Korobov, S. Korpar, E. Kovalenko, R. Kowalewski, T. M. G. Kraetzschmar, P. Križan, P. Krokovny, T. Kuhr, Y. Kulii, J. Kumar, M. Kumar, R. Kumar, K. Kumara, T. Kunigo, A. Kuzmin, Y.-J. Kwon, S. Lacaprara, Y.-T. Lai, T. Lam, L. Lanceri, J. S. Lange, M. Laurenza, R. Leboucher, F. R. Le Diberder, M. J. Lee, D. Levit, C. Li, L. K. Li, Y. Li, Y. B. Li, J. Libby, Y.-R. Lin, M. Liu, Q. Y. Liu, Z. Q. Liu, D. Liventsev, S. Longo, T. Lueck, C. Lyu, Y. Ma, M. Maggiora, S. P. Maharana, R. Maiti, S. Maity, G. Mancinelli, R. Manfredi, E. Manoni, M. Mantovano, D. Marcantonio, S. Marcello, C. Marinas, L. Martel, C. Martellini, A. Martini, T. Martinov, L. Massaccesi, M. Masuda, K. Matsuoka, D. Matvienko, S. K. Maurya, J. A. McKenna, R. Mehta, F. Meier, M. Merola, F. Metzner, C. Miller, M. Mirra, S. Mitra, K. Miyabayashi, H. Miyake, R. Mizuk, G. B. Mohanty, N. Molina-Gonzalez, S. Mondal, S. Moneta, H.-G. Moser, M. Mrvar, R. Mussa, I. Nakamura, K. R. Nakamura, M. Nakao, Y. Nakazawa, A. Narimani Charan, M. Naruki, D. Narwal, Z. Natkaniec, A. Natochii, L. Nayak, M. Nayak, G. Nazaryan, M. Neu, C. Niebuhr, S. Nishida, S. Ogawa, Y. Onishchuk, H. Ono, Y. Onuki, P. Oskin, F. Otani, P. Pakhlov, G. Pakhlova, A. Panta, S. Pardi, K. Parham, H. Park, S.-H. Park, B. Paschen, A. Passeri, S. Patra, S. Paul, T. K. Pedlar, R. Peschke, R. Pestotnik, M. Piccolo, L. E. Piilonen, G. Pinna Angioni, P. L. M. Podesta-Lerma, T. Podobnik, S. Pokharel, C. Praz, S. Prell, E. Prencipe, M. T. Prim, H. Purwar, P. Rados, G. Raeuber, S. Raiz, N. Rauls, M. Reif, S. Reiter, M. Remnev, I. Ripp-Baudot, G. Rizzo, M. Roehrken, J. M. Roney, A. Rostomyan, N. Rout, G. Russo, D. A. Sanders, S. Sandilya, A. Sangal, L. Santelj, Y. Sato, V. Savinov, B. Scavino, C. Schmitt, C. Schwanda, M. Schwickardi, Y. Seino, A. Selce, K. Senyo, J. Serrano, M. E. Sevior, C. Sfienti, W. Shan, X. D. Shi, T. Shillington, T. Shimasaki, J.-G. Shiu, D. Shtol, A. Sibidanov, F. Simon, J. B. Singh, J. Skorupa, R. J. Sobie, M. Sobotzik, A. Soffer, A. Sokolov, E. Solovieva, S. Spataro, B. Spruck, M. Starič, P. Stavroulakis, S. Stefkova, R. Stroili, M. Sumihama, K. Sumisawa, W. Sutcliffe, H. Svidras, M. Takizawa, U. Tamponi, S. Tanaka, K. Tanida, F. Tenchini, O. Tittel, R. Tiwary, D. Tonelli, E. Torassa, K. Trabelsi, I. Tsaklidis, M. Uchida, I. Ueda, Y. Uematsu, K. Unger, Y. Unno, K. Uno, S. Uno, P. Urquijo, Y. Ushiroda, S. E. Vahsen, R. van Tonder, K. E. Varvell, M. Veronesi, A. Vinokurova, V. S. Vismaya, L. Vitale, V. Vobbilisetti, R. Volpe, B. Wach, M. Wakai, S. Wallner, E. Wang, M.-Z. Wang, X. L. Wang, Z. Wang, A. Warburton, S. Watanuki, C. Wessel, E. Won, X. P. Xu, B. D. Yabsley, S. Yamada, W. Yan, S. B. Yang, J. Yelton, J. H. Yin, K. Yoshihara, C. Z. Yuan, Y. Yusa, B. Zhang, V. Zhilich, Q. D. Zhou, X. Y. Zhou, V. I. Zhukova, and R. Žlebčík

(The Belle II Collaboration)

We present GFlaT, a new algorithm that uses a graph-neural-network to determine the flavor of neutral B mesons produced in $\Upsilon(4S)$ decays. It improves previous algorithms by using the information from all charged final-state particles and the relations between them. We evaluate its performance using B decays to flavor-specific hadronic final states reconstructed in a $362\,\mathrm{fb}^{-1}$ sample of electron-positron collisions collected at the $\Upsilon(4S)$ resonance with the Belle II detector at the SuperKEKB collider. We achieve an effective tagging efficiency of $(37.40 \pm 0.43 \pm 0.36)\,\%$, where the first uncertainty is statistical and the second systematic, which is 18% better than the previous Belle II algorithm. Demonstrating the algorithm, we use $B^0 \to J/\psi K^0_S$ decays to measure the mixing-induced and direct CP violation parameters, $S = (0.724 \pm 0.035 \pm 0.014)$ and $C = (-0.035 \pm 0.026 \pm 0.013)$.

PACS numbers:

I. INTRODUCTION

In the standard model, CP violation arises from an irreducible complex phase in the Cabibbo-Kobayashi-Maskawa (CKM) matrix [1]. Measurements of mixing-induced CP violation in B^0 meson decays constrain the values of the CKM-unitarity-triangle angles ϕ_1 and ϕ_2,[1] helping us probe for sources of CP violation beyond the standard model. For example, we learn ϕ_1 from $B^0 \to J/\psi K^0$ [2–4] and ϕ_2 from $B^0 \to (\pi\pi)^0$ [5–7], $(\rho\rho)^0$ [8–10]. These measurements require knowledge of the neutral B meson flavor. At B factory experiments, B^0 and $\overline{B}^0$ mesons are produced in pairs from e^+e^- collisions at the $\Upsilon(4S)$ resonance. Since their states are entangled, tagging the flavor of one of the mesons, $B_{\rm tag}$, at the time of its decay determines the flavor of the other one, $B_{\rm sig}$, at the same time [11, 12].

The Belle II [13] experiment reported results using a flavor tagger [14–16] based on algorithms developed by the Belle and *BABAR* experiments [2, 17]. It uses the kinematic, topology, particle-identification, and charge information of charged final-state particles in the $B_{\rm tag}$ decay to infer if they originated from categories of flavor-specific decays. For instance, a charged particle is assigned as being a μ^+ in a $B^0 \to D\mu^+\nu_\mu X$ decay or a K^+ in the subsequent $D \to K^+ Y$ decay, the charge of which correlates to the $B_{\rm tag}$ flavor. This category-based flavor tagger selects the most probable assignment in each category, discards all other possibilities in that category, and then combines the probabilities of the selected assignments to predict the $B_{\rm tag}$ flavor.

In this paper, we present a new algorithm, the graph-neural-network flavor tagger, GFlaT, which uses a dynamic-graph-convolutional-neural-network [18] to combine the information from all charged final-state particles. It improves flavor tagging by accounting for the discarded information in the category-based flavor tagger and correlations between information from final-state particles.

To demonstrate GFlaT, we measure the CP parameters of $B^0 \to J/\psi K^0_S$ from which we calculate ϕ_1. The probability density to observe $B_{\rm sig}$ decay at a time Δt from when $B_{\rm tag}$ decays with flavor $q_{\rm tag}$ (1 for B^0, -1 for $\overline{B}^0$) is

$$P(\Delta t, q_{\rm tag}) = \frac{e^{-|\Delta t|/\tau}}{4\tau}\big\{1 + q_{\rm tag}(1-2w)[S\sin(\Delta m_d \Delta t) - C\cos(\Delta m_d \Delta t)]\big\}, \quad (1)$$

where $q_{\rm tag}$ is determined by the flavor tagger, w is the probability to wrongly determine it, τ is the B^0 lifetime, and Δm_d is the difference of masses of the B^0 mass eigenstates.[2] Here S and C, the parameters of interest, quantify mixing-induced and direct CP violation, respectively. In the standard model, $S = \sin 2\phi_1$ and $C = 0$ to good precision [19–21]. At B factories, the B mesons are boosted and have significant momentum in the lab frame, so Δt is determined from the relative displacement of their decay vertices.

To measure CP parameters in tagged B^0 decays, we must know w. We determine it from events with the flavor-specific $B_{\rm sig}$ decaying as $B^0 \to D^{(*)-}\pi^+$, for which

$$P(\Delta t, q_{\rm sig}, q_{\rm tag}) = \frac{e^{-|\Delta t|/\tau}}{4\tau}\big\{1 - q_{\rm sig} q_{\rm tag}(1-2w)\cos(\Delta m_d \Delta t)\big\}, \quad (2)$$

where $q_{\rm sig}$ equals the charge of the pion from the $B_{\rm sig}$ decay, neglecting the $\mathcal{O}(10^{-4})$ wrong-sign contribution

[1] These angles are also known as β and α.

[2] We use a system of units in which $\hbar = c = 1$ and mass and frequency have the same dimension.

EUROPEAN ORGANISATION FOR NUCLEAR RESEARCH (CERN)

CERN-EP-2024-051
February 28, 2024

K^0_S meson production in inelastic p+p interactions at 31, 40 and 80 GeV/c beam momentum measured by NA61/SHINE at the CERN SPS

The NA61/SHINE Collaboration

Measurements of K^0_S meson production via its $\pi^+\pi^-$ decay mode in inelastic p+p interactions at incident projectile momenta of 31, 40 and 80 GeV/c ($\sqrt{s_{NN}} = 7.7, 8.8$ and 12.3 GeV, respectively) are presented. The data were recorded by the NA61/SHINE spectrometer at the CERN Super Proton Synchrotron. Double-differential distributions were obtained in transverse momentum and rapidity. The mean multiplicities of K^0_S mesons were determined to be $(5.95 \pm 0.19(stat) \pm 0.22(sys)) \times 10^{-2}$ at 31 GeV/c, $(7.61 \pm 0.13(stat) \pm 0.31(sys)) \times 10^{-2}$ at 40 GeV/c and $(11.58 \pm 0.12(stat) \pm 0.37(sys)) \times 10^{-2}$ at 80 GeV/c. The results on K^0_S production are compared with model calculations (EPOS1.99, SMASH 2.0 and PHSD) as well as with published data from other experiments.

Contents

Estimation of the electromagnetic field in intermediate-energy heavy-ion collisions

Hidetoshi Taya,[1,*] Toru Nishimura,[2,3] and Akira Ohnishi[3]

[1] *RIKEN iTHEMS, RIKEN, Wako 351-0198, Japan*
[2] *Department of Physics, Osaka University, Toyonaka, Osaka, 560-0043, Japan*
[3] *Yukawa Institute for Theoretical Physics, Kyoto University, Kyoto, 606-8317, Japan*

We estimate the spacetime profile of the electromagnetic field in head-on heavy-ion collisions at intermediate collision energies $\sqrt{s_{\rm NN}} = \mathcal{O}(3\text{ - }10\text{ GeV})$. Using a hadronic cascade model (JAM; Jet AA Microscopic transport model), we numerically demonstrate that the produced field has strength $eE = \mathcal{O}((30\text{ - }60\text{ MeV})^2)$, which is supercritical to the Schwinger limit of QED and is non-negligibly large compared even to the hadron/QCD scale, and survives for a long time $\tau = \mathcal{O}(10\text{ fm}/c)$ due to the baryon stopping. We show that the produced field is nonperturbatively strong in the sense that the nonperturbativity parameters (e.g., the Keldysh parameter) are sufficiently large, which is in contrast to high-energy collisions $\sqrt{s_{\rm NN}} \gtrsim 100$ GeV, where the field is merely perturbative. Our results imply that the electromagnetic field may have phenomenological impacts on hadronic/QCD processes in intermediate-energy heavy-ion collisions and that heavy-ion collisions can be used as a new tool to explore strong-field physics in the nonperturbative regime.

I. INTRODUCTION

Super dense matter, such as that realized inside a neutron star or even denser, can be produced on Earth by colliding heavy ions at intermediate collision energies $\sqrt{s_{\rm NN}} = \mathcal{O}(3\text{ - }10\text{ GeV})$. Such collision experiments have been performed in the Beam Energy Scan program at RHIC [1] and are planned worldwide (e.g., FAIR [2], NICA [3], HIAF [4], J-Parc-HI [5]) to reveal the extreme form of matter in the dense limit and to develop a better understanding of strong interaction, or quantum chromodynamics (QCD). These experimental programs have motivated various theoretical studies, which are mainly aimed at investigating the consequences of the high-density matter and the dynamics of how it can be created during the collisions, e.g., novel phases of QCD at finite density (see Ref. [6] for a review) and the development of various transport models to simulate the real-time collision dynamics such as RQMD [7], UrQMD [8, 9], JAM [10], and SMASH [11].

The purpose of this paper is, rather than pursuing the high-density physics as previously discussed, to point out that a strong electromagnetic field can be created in intermediate-energy heavy-ion collisions. The generation of such a strong electromagnetic field is of interest not only to hadron/QCD physics but also to the area of strong-field physics. For hadron/QCD physics, electromagnetic observables such as di-lepton yields [12–15], which are promising probes of nontrivial processes induced by the high-density matter, are naturally affected by the presence of a strong electromagnetic field. A correct estimation of the electromagnetic-field profile (and also its implementation into transport-model simulations; cf. Ref. [16, 17]) is, therefore, important when extracting/interpreting signals of the high-density matter from the actual experimental data. As for strong-field physics, the generation of a strong electromagnetic field would provide a unique and novel opportunity to study quantum electrodynamics (QED) in the nonperturbative regime beyond the Schwinger limit $eE_{\rm cr} := m_e^2 = (0.511\text{ MeV})^2$ (with $e = |e|$ being the elementary electric charge, E electric field strength, and m_e the electron mass). Currently, strong-field physics is driven mainly by high-power lasers (see, e.g., Refs. [18, 19] for reviews). The focused laser intensity of $I = 1\times10^{23}$ W/cm^2 (corresponding to $E \approx 10^{-3}\,E_{\rm cr}$) is the current world record [20], which is envisaged to be surpassed by the latest and future facilities such as Extreme Light Infrastructure (ELI) $I = \mathcal{O}(10^{25}$ W/cm$^2)$ [21]. Although the laser intensity is growing rapidly, it is and will remain, for at least the next decade, several orders of magnitude below the Schwinger limit $E_{\rm cr}$. Therefore, it is difficult to study strong-field phenomena with current lasers. This means that a novel method or physical system to realize a strong electromagnetic field is highly demanded.

There exist a number of studies on the generation of a strong electromagnetic field at low- and high-energies both theoretically and experimentally. Let us briefly review them, so as to clarify our motivation to go to the intermediate energy. At low energies, due to the baryon stopping (i.e., the Landau picture [22, 23]), the collided ions stick together at the collision point and form up a gigantic ion with large atomic number $Z = \mathcal{O}(100)$, and thereby creates a strong Coulomb electric field of the order of $eE \sim (e^2/4\pi)Z/R^2 = \mathcal{O}((20\text{ MeV})^2)$, where $R = \mathcal{O}(10\text{ fm})$ is the typical radius of the gigantic ion. The produced field is weak compared to the hadron/QCD scale but is far surpassing the Schwinger limit of QED. Thus, it is expected to induce intriguing nonlinear QED processes such as the vacuum decay (see Ref. [24] for a recent analysis), experimental investigation of which has been done around 1980s but is not conclusive yet (see, e.g., Ref. [25] for possible interpretations of the experimental results). On the other hand, at high energies, the Bjorken picture [26] is valid rather than the Landau picture. The colliding ions penetrate with each other

* hidetoshi.taya@riken.jp

On the significance of radiative corrections on measurements of the EMC effect

S. Moran,[1] M. Arratia,[1] J. Arrington,[2] D. Gaskell,[3] and B. Schmookler[1]

[1] *Department of Physics and Astronomy, University of CA, Riverside, California 92521, USA*
[2] *Lawrence Berkeley National Laboratory, Berkeley, CA 94720, USA*
[3] *Thomas Jefferson National Accelerator Facility, Newport News, VA 23606, USA*

(Dated: February 28, 2024)

Analyzing global data on the EMC effect, which denotes differences in parton distribution functions in nuclei compared to unbound nucleons, reveals tensions. Precise measurements at Jefferson Lab, studying both x and A dependence, show systematic discrepancies among experiments, making the extraction of the A dependence of the EMC effect sensitive to the selection of datasets. By comparing various methods and assumptions used to calculate radiative corrections, we have identified differences that, while not large, significantly impact the EMC ratios and show that using a consistent radiative correction procedure resolves this discrepancy, leading to a more coherent global picture, and allowing for a more robust extraction of the EMC effect for infinite nuclear matter.

INTRODUCTION

Precision measurement of deep-inelastic scattering (DIS) from nucleons and nuclei allows for an extraction of parton distribution functions (pdfs). Early measurements of the nuclear pdfs demonstrated that the quark distributions in iron were not simply the sum of the distribution arising from its constituent protons and neutrons [1]. Since the initial observation of this "EMC effect", additional measurements have been made for a wide range of nuclei [2–8] and many different explanations have been proposed to explain this observation [6, 9–13]. One of these measurements [4] demonstrated an unexpected, non-trivial dependence on nuclear structure in light nuclei [4] which corresponded to a similar dependence in the number of short-range correlations (SRCs) [14, 15], renewing interest in precision measurements of the A dependence of the EMC effect.

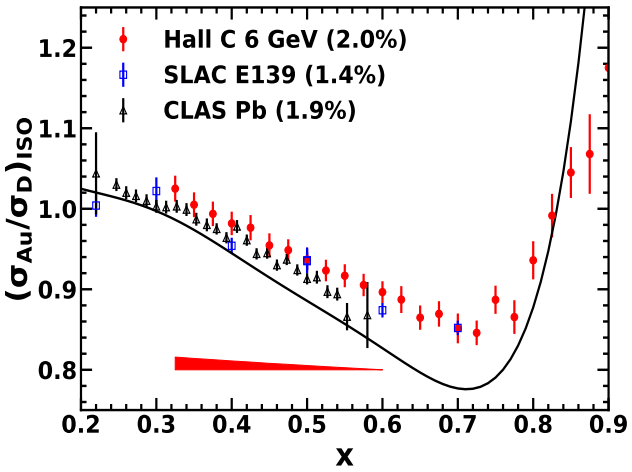

FIG. 1. EMC ratios for gold and lead [2, 5, 6] after applying uniform isoscalar corrections from [6]. The number in parentheses is the normalization uncertainty, the solid curve is the parameterization of Ref. [2], and the red band indicates the correlated systematic uncertainty for Ref. [6].

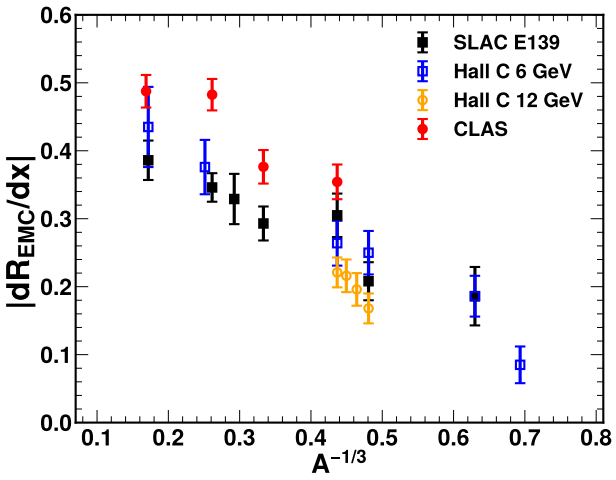

FIG. 2. EMC slopes from world's data, with the common isoscalar correction from Ref. [6] applied to all data sets.

Figure 1 shows the EMC ratios from various experiments for heavy (A≈200) nuclei after applying consistent isoscalar corrections [6]. The size of the EMC effect is typically parameterized by taking the slope of the EMC ratios for $0.3 \leq x \leq 0.7$, and a comparison of world data on the EMC slopes is shown in Figure 2. As noted in Ref. [6] the CLAS slopes [5] are systematically higher, even when applying identical isoscalar corrections. Some fraction of the experimental uncertainty will be correlated across the slopes from a given measurement, as they all use common deuterium data. However, the CLAS slopes are systematically higher by roughly 0.10, much larger than the total quoted uncertainties of ∼0.02.

Because the CLAS measurement [5] includes only heavier nuclei, the inclusion of this data yields a significant change in the required A dependence over the full range of nuclei measured [6]. Even excluding ^{3}He, the inclusion of the CLAS data yields a significant difference in the A dependence. A linear fit of the EMC slope vs $A^{-1/3}$ for the data shown in Fig. 2 (excluding ^{3}He and